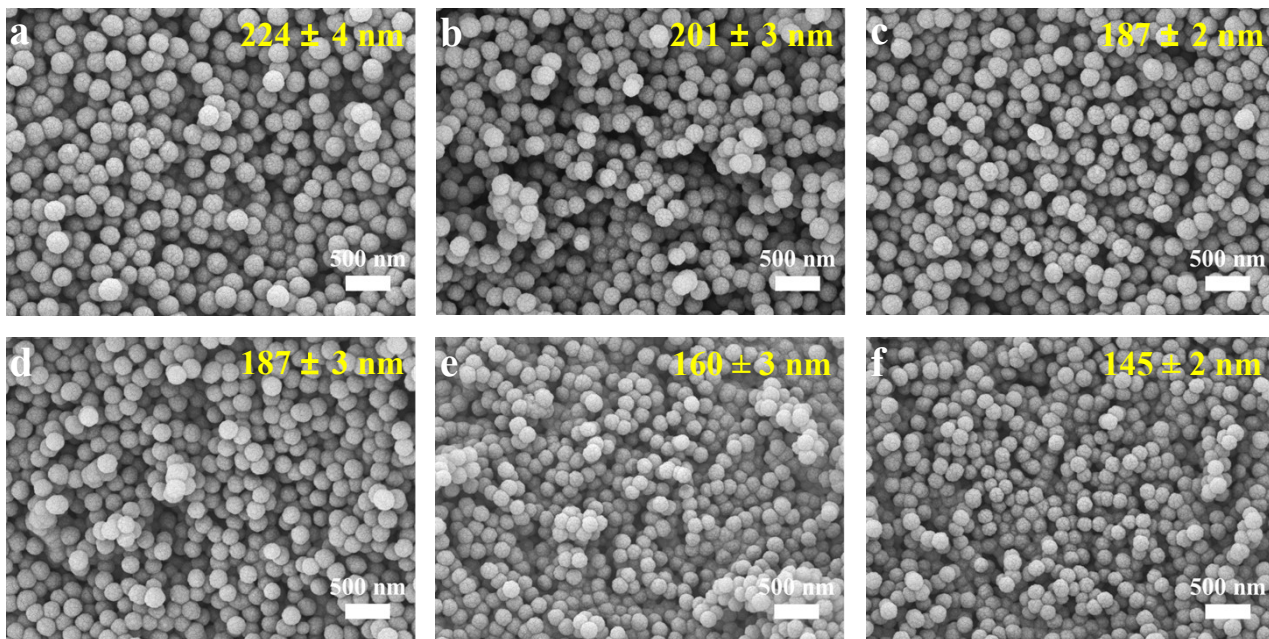
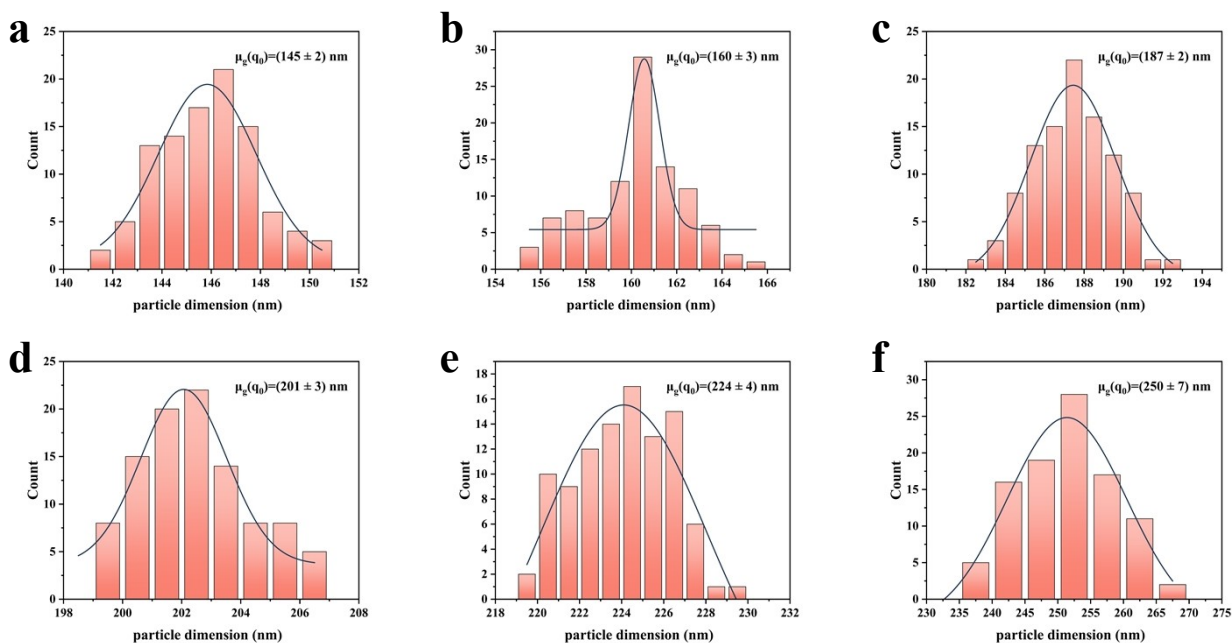


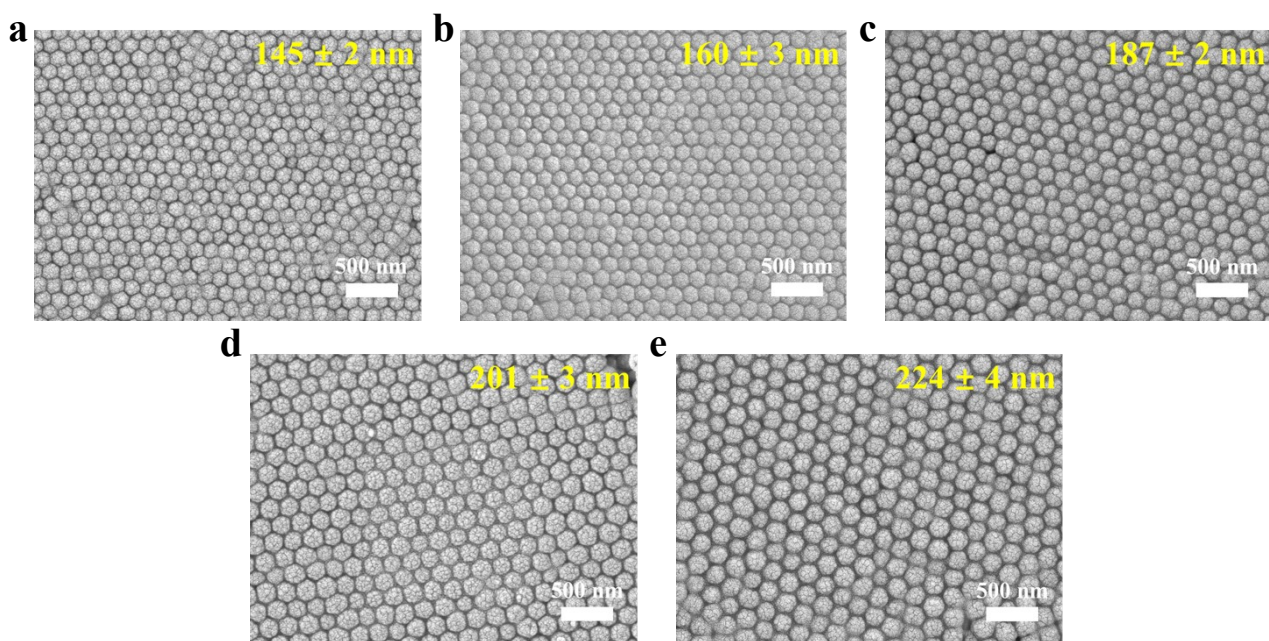
1 **Supporting Information**
2 **A Fluorescence Sensor Utilizing 3D COF Photonic Crystals for Enhanced**
3 **Detection of TNP**
4



5
6 **Figure S1.** FE-SEM images of TAPB-BTCA-COF particles of (a) 224 ± 4 nm, (b) 201 ± 3 nm, (c)
7 187 ± 2 nm, (d) 187 ± 3 nm, (e) 160 ± 3 nm, and (f) 145 ± 2 nm.



8
9 **Figure S2.** The particle size distribution of COF nanoparticles with (a) 145 ± 2 nm,
10 $(b) 160 \pm 3$ nm, (c) 187 ± 2 nm, (d) 201 ± 3 nm, (e) 224 ± 4 nm, and (f) 250 ± 7 nm.

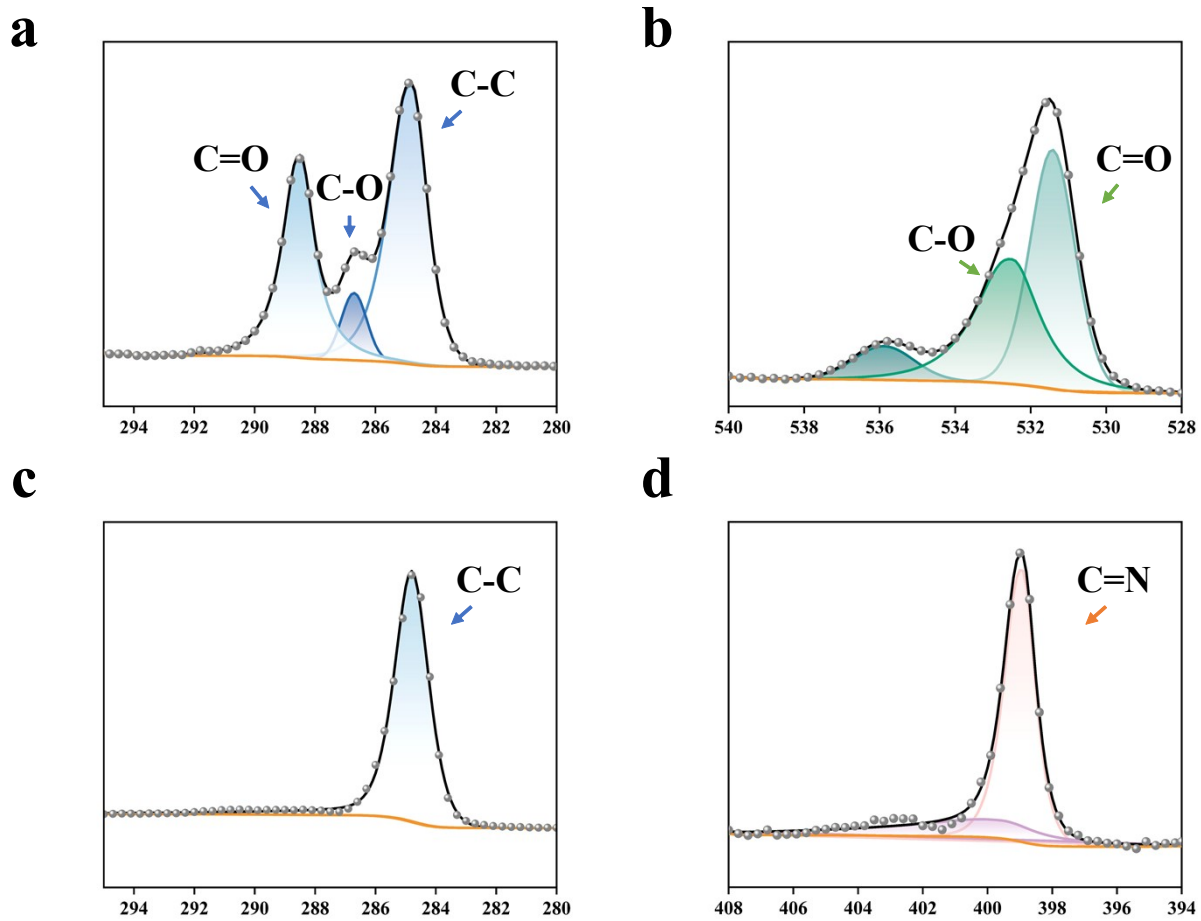


11

12 **Figure S3.** FE-SEM images of superstructures comprising TAPB-BTCA-COF particles of (a) $145 \pm$

13 2 nm, (b) 160 ± 3 nm, (c) 187 ± 2 nm, (d) 201 ± 3 nm and (e) 224 ± 4 nm.

14

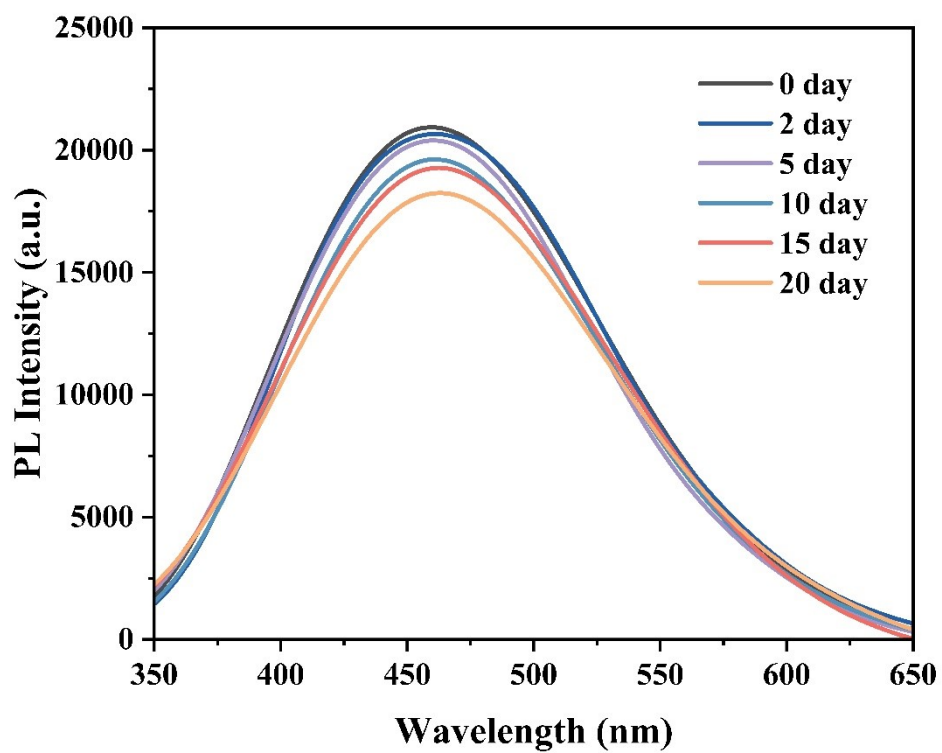


15

16 **Figure S4.** High-resolution XPS spectrum of (a) C 1s, (b) O 1s of FPTA NPs and (c) C 1s , (d) N 1s

17

of COF PhCs.



18

19

Figure S5. PL spectra changes of PhCs-FPTA NPs with time.

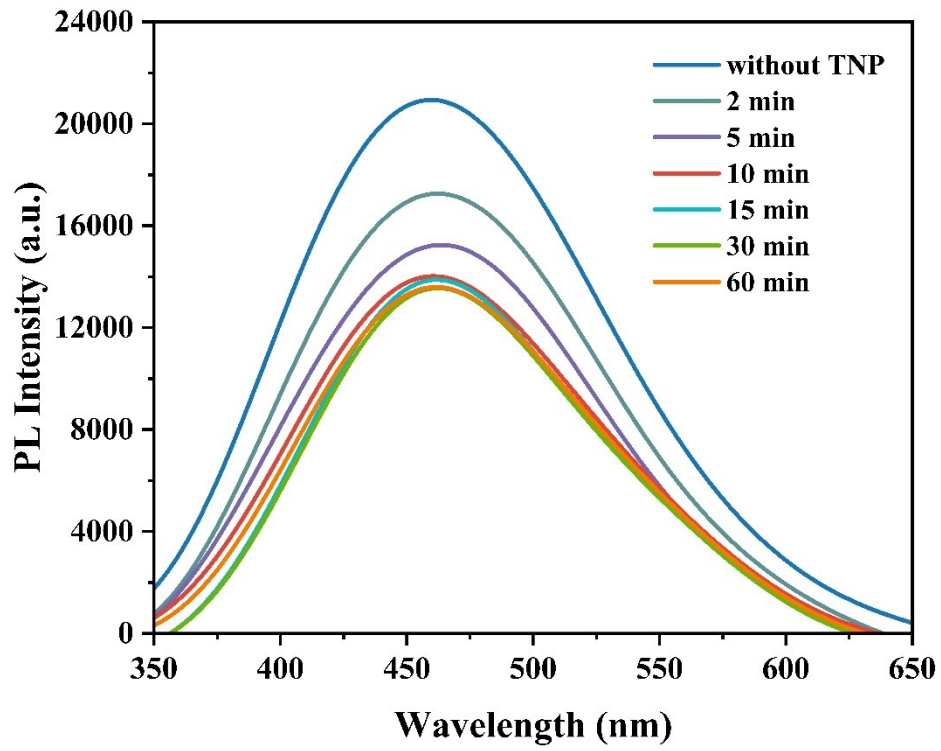
20

21

22

Table S1. Comparison with other mostprevious works for the detection of TNP

No.	Detectable substance	Linear range	LOD	REF
1	GODs	0.1–15 μM	91 nM	1
2	Nph-An	0– 1×10^{-4} M	470 nM	2
3	N-GQDs	0–4 μM	420 nM	3
4	CQD	0.1–15.8 μM	27 nM	4
5	Luminol-SiNPs	0.08–1 μM	22.4 nM	5
6	Zn (II) -MOF	0–25 μM	0.32 μM	6
7	PEI-G PNP	0.05–70 μM	26 nM	7
8	GQD-50	0–200 μM	1.2 μM	8
9	RP-HPLC	0.22–1.1 μM	390 nM	9
10	Electrochemical	28.4–436 μM	43.6 nM	10
11	PhCs-based fluorescence sensor	100–1000 nM	20.7 nM	This work



25

26 **Figure S6.** Time response of the PhC-based PL sensor for the detection of 500 nM TNP.

27

28

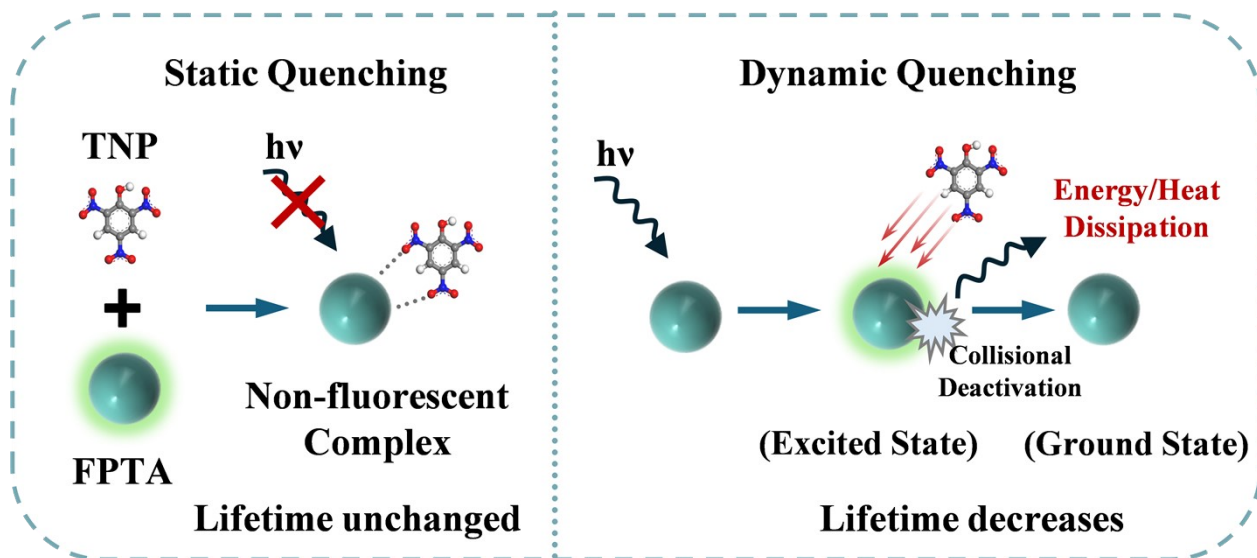
Table S2. Detection of TNP in simulated organic wastewater

Sample	Spiked malathion (nM)	Measured (nM)	Recovery (%)	RSD (%)
	0	N/A*	—	—
	50	50.6	101.2	3.56
Simulated organic wastewater	100	99.5	99.5	2.26
	500	505.4	101.1	2.73
	1000	987.3	98.7	4.3
	2000	2067.3	103.4	4.09

30 *The quenching index was lower than 5 %, so we assumed that TNP were not detected.

31

32



33

34

Figure S7. Illustration of the proposed fluorescence quenching mechanisms.

35

36 **References**

- 37 1. Z. Li, Y. Wang, Y. Ni and S. Kokot, A sensor based on blue luminescent graphene quantum dots
38 for analysis of a common explosive substance and an industrial intermediate, 2,4,6-trinitrophenol,
39 *Spectrochimica Acta Part A: Molecular and Biomolecular Spectroscopy*, 2015, 137, 1213-1221.
- 40 2. H. Ma, C. He, X. Li, O. Ablikim, S. Zhang and M. Zhang, A fluorescent probe for TNP detection
41 in aqueous solution based on joint properties of intramolecular charge transfer and aggregation-
42 induced enhanced emission, *Sensors and Actuators B: Chemical*, 2016, 230, 746-752.
- 43 3. M. Kaur, S. K. Mehta and S. K. Kansal, Nitrogen doped graphene quantum dots: Efficient
44 fluorescent chemosensor for the selective and sensitive detection of 2,4,6-trinitrophenol, *Sensors and*
45 *Actuators B: Chemical*, 2017, 245, 938-945.
- 46 4. Y. Z. Fan, Q. Tang, S. G. Liu, Y. Z. Yang, Y. J. Ju, N. Xiao, H. Q. Luo and N. B. Li, A
47 smartphone-integrated dual-mode nanosensor based on novel green-fluorescent carbon quantum dots
48 for rapid and highly selective detection of 2,4,6-trinitrophenol and pH, *Applied Surface Science*,
49 2019, 492, 550-557.
- 50 5. W. Qi, Y. Fu, H. He, M. Zhao, D. Wu, L. Qi, L. Hu and R. Li, Electrochemiluminescence
51 resonance energy transfer for both “turn-off” detection of 2,4,6-trinitrophenol and “turn-on”
52 detection of lidocaine hydrochloride using luminol-doped silica nanoparticles, *Sensors and Actuators*
53 *B: Chemical*, 2019, 287, 445-452.
- 54 6. T. Wiwasuku, J. Boonmak, K. Siritwong, V. Ervithayasuporn and S. Youngme, Highly sensitive
55 and selective fluorescent sensor based on a multi-responsive ultrastable amino-functionalized Zn(II)-
56 MOF for hazardous chemicals, *Sensors and Actuators B: Chemical*, 2019, 284, 403-413.
- 57 7. S. G. Liu, D. Luo, N. Li, W. Zhang, J. L. Lei, N. B. Li and H. Q. Luo, Water-Soluble

58 Nonconjugated Polymer Nanoparticles with Strong Fluorescence Emission for Selective and
59 Sensitive Detection of Nitro-Explosive Picric Acid in Aqueous Medium, ACS Applied Materials &
60 Interfaces, 2016, 8, 21700-21709.

61 8. D. Mukherjee, P. Das, S. Kundu and B. Mandal, Engineering of graphene quantum dots by
62 varying the properties of graphene oxide for fluorescence detection of picric acid, Chemosphere,
63 2022, 300.

64 9. S. M. Ünsal and E. Erkan, Development and validation of a new RP-HPLC method for organic
65 explosive compounds, Turk. J. Chem, 2022, 46, 923-928.

66 10. R. Manikandan, B. Kavitha, S. Rani and N. Senthil Kumar, Quantification of Picric Acid on
67 Nanosphere Polypyrrole Modified Electrode by Stripping Voltammetry Method, J. Mex. Chem. Soc,
68 2019, 63, 146-154.